ISSN No: 2348-4845
International Journal & Magazine of Engineering, Technology, Management and Research
A Peer Reviewed Open Access International Journal

PV and Battery Energy Storage System Along With SOC Control Method for a Dual-Inverter-Fed Open-End Winding Induction Motor Drive

M.Krishna Priya
PG Schloar,
Department of EEE,
Visvodaya Engineering College.

V. Madhu Sudhna Reddy, M.Tech, Ph.D
Associate Professor,
Department of EEE,
Visvodaya Engineering College.

Abstract:

This paper introduces an incorporated solution for a photo-voltaic (PV) and battery energy storage- fed water-pump drive framework, which utilizes an open-end winding induction machine (OEWIM). The double inverter-bolstered OEWIM drive accomplishes the usefulness of a three-level inverter and obliges low esteem dc-transport voltage. This aides in an ideal course of action of PV modules, which could keep away from expansive strings and aides in enhancing the PV execution with wide transfer speed of working voltage. It additionally decreases the voltage rating of the dc-join capacitors and exchanging gadgets utilized as a part of the framework.

The proposed control method accomplishes a reconciliation of both most extreme force point following and SOC control for the proficient usage of the PV boards and the engine. The proposed control plan obliges the detecting of PV voltage and current just. In this manner, the framework obliges less number of sensors. All the diagnostic, recreation, and test consequences of this work under distinctive ecological conditions are exhibited in this paper.

INTRODUCTION:

An induction motor can run only at its rated speed when it is connected directly to the main supply. However, many applications need variable speed operations. This is felt the most in applications where input power is directly proportional to the cube of motor speed. In applications like the induction motor-based centrifugal pump, a speed reduction of 20% results in an energy savings of approximately 50%. Driving and controlling the induction motor efficiently are prime concerns in today's energy conscious world. With the advancement in the semiconductor fabrication technology, both the size and the price of semiconductors have gone down drastically.

This means that the motor user can replace an energy inefficient mechanical motor drive and control system with a Variable Frequency Drive (VFD). The VFD not only controls the motor speed, but can improve the motor's dynamic and steady state characteristics as well. In addition, the VFD can reduce the system's average energy consumption. Although various induction motor control techniques are in practice today, the most popular control technique is by generating variable frequency supply, which has constant voltage to frequency ratio. This technique is popularly known as VF control. Generally used for open-loop systems, VF control caters to a large number of applications where the basic need is to vary the motor speed and control the motor efficiently. It is also simple to implement and cost effective.

II. BASIC:

Topology of A Dual inverter-fed OPEN-END winding motor drive with Two DC SOURCES Fig. 1 presents basic structure of a dual inverter-fed open end winding induction motor drive with two standard voltage source inverters with pulse width modulation, which are supplied by two separate dc-link sources with voltages Vdc1 and Vdc2 [3]. Separate dc supply is used for each inverter to block the flow of third harmonic currents.

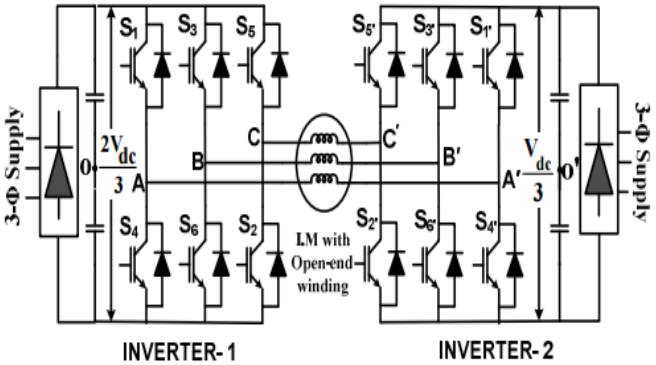

Fig 1 Dual two-level inverter fed open-end winding topology

ISSN No: 2348-4845
International Journal & Magazine of Engineering, Technology, Management and Research
A Peer Reviewed Open Access International Journal

The dual-inverter fed open-end winding induction motor configuration offers an elegant alternative to the existing multilevel inverter configurations such as NPC, Flying capacitor and the cascaded H-bridge for induction motor drives [1]-[8]. One of the advantages of open-end winding configuration is that multilevel inversion is achieved by using the conventional two two-level inverters as a basic building block. A power circuit configuration to realize a four-level inverter with open-end winding induction motor, which employs two inverters with DC-link voltages in the ratio of 2:1 is reported in [4], is shown in Fig. 1. To suppress the zero-sequence components in the motor phases, each inverter is operated with an isolated DC power supply.

II. MODELING OF THE PROPOSED SYSTEM:

A proposed configuration of the solar PV-powered pumping system is shown in Fig. 2, which comprises of: 1) solar PV array; 2) dual-inverter namely Inverters I and II; 3) three-phase OEWIM with pump load; and 4) controller block which consists of MPPT and DSAZE PWM algorithm. These components are described in detail in the following sections.

A.PV Source Model:

The PV source was modeled by using PV cell current–voltage characteristic equation as follows [29]:

$$i_{pvcell} = i_L - i_0 \left(e^{\frac{q\left(v_{pvcell} + i_{pvcell} R_s\right)}{nkT}} - 1 \right) \quad (1)$$

where ipvcell is PV cell current,
iL is photocurrent,
i0 is diode saturation current,
n is diode quality or ideality factor,
k is Boltzmann constant,
q is electron charge,
T is panel operating temperature in Kelvin,
Rs is PV cell series resistance, and
Vpvcell is PV cell voltage (V).

The output of PV source is connected to inverter with dc-bus capacitance Cpv . By applying KCL at input of the inverter [from Fig. 2]

ipv = ic + iinv ipv = Cpv dvpv/ dt + iinv . (2)

Integral solution of (2) is the voltage vpv across capacitance Cpv , which is used by the PV model to calculate the PV source current. The inverter current iinv is the current drawn by Inverters I and II. Further dual inverter has two series connected equal value capacitors across the dc link. These capacitors share equal voltage with respect to the common point “o” as shown in Fig. 2.

B.Modular Three-Level Dual-Inverter Model

Dual inverter used in the proposed configuration is modeled using switching functions [30]. To model dual inverter, switching function SW (where W can be A, B, C, A’, B’ or C’ depending on the phase and number of inverter) requires the logic generated from the PWM controller. It has value 1 and –1 which represents turn ON of top and bottom switch, respectively, for the given leg or phase of the inverter. The modular dual inverter shown in Fig. 2 consists of six poles (a, b, c, a’, b’, and c’) and 12 switches (two switches per pole). The value of the pole voltages in a particular phase can be ±Vpv /2 depending on the switch (whether top or bottom) is turned ON. If top switch of phase “a”, S1 is turned ON, the pole voltage vao is +Vpv /2 and when bottom switch of phase “a”, S4 is turned ON, then the pole voltage vao is −Vpv /2. Thus, pole voltage of Inverter I can be given as

vao = SA Vpv /2 ; vbo = SB Vpv /2 ; vco = SC Vpv /2. (3)

Similarly, pole voltage of Inverter II can be given as

Va`o = SA` Vpv/ 2 ; vb`o = SB` Vpv/ 2 ; vc`o = SC` Vpv/ 2 . (4)

The motor phase voltage vaa` is given by

vaa = Vpv/ 2[2/3 (SA − SA`) – 1/3 ((SB – SB`)+(SC – SC`))] . (5)

Similarly, the other phase voltages vbb,vcc of the inverter output can be derived for the system. Further, the input inverter current iinv can also be derived using switching functions. Current flowing through Inverter I is given by

iinv1 = 1/ 2 (SA + 1)iaa + 1/ 2 (SB + 1)ibb + 1/ 2 (SC + 1)icc. (6)

Current flowing through the Inverter II is given by

ISSN No: 2348-4845
International Journal & Magazine of Engineering, Technology, Management and Research
A Peer Reviewed Open Access International Journal

iinv2 = 1 /2 (SA + 1)(−iaa) + 1/ 2 (SB + 1)(−ibb) + 1/ 2 (SC + 1)(−icc). (7)

The net current flowing through the dual inverter is

iinv = 1/ 2 iaa(SA − SA) + 1/ 2 ibb(SB − SB) + 1/ 2 icc(SC − SC). (8)

Thus, the previous values of phase voltage and current can be used by the Simulink model of OEWIM, which is discussed in the next section.

B.OEWIM Model:

An OEWIM [28] is obtained by opening the neutral point of the star-connected stator windings of a normal three-phase IM. The winding diagram of three-phase OEWIM is shown in Fig. 3.For modeling and analysis, the de-coupled form of OEWIM is considered. For transforming the stator (φ = θ) and the rotor parameters (φ = β) to decoupled form, the transformation matrix used is given as follows:

$$\begin{bmatrix} x_{qy} \\ x_{dy} \\ x_{0y} \end{bmatrix} = \frac{2}{3} \begin{bmatrix} \cos\phi & \cos(\phi - 2\pi/3) & \cos(\phi + 2\pi/3) \\ \sin\phi & \sin(\phi - 2\pi/3) & \sin(\phi + 2\pi/3) \\ 1/2 & 1/2 & 1/2 \end{bmatrix} \begin{bmatrix} x_{aa'} \\ x_{bb'} \\ x_{cc'} \end{bmatrix} \quad (9)$$

where θ is the angle between the stator as-axis and the quadrature (q) axis, β is the angle between rotor ar-axis and the q-axis, also β = θ − θr , θr is the angle between rotor ar-axis and stator asaxis (see Fig. 3), parameter x can be either voltage "v" or current "i" or flux linkage "λ" and subscript parameter y can be "s" or "r." The subscript "s" denotes the parameters of stator and the subscript "r" denotes the parameters of rotor.

The dynamic d–q model of an OEWIM is described by

vqs = Rs iqs + ω(Lls ids + Lm (ids + i dr)) + pλqs (10)

vds = Rs ids − ω(Lls iqs + Lm (iqs + i qr)) + pλds (11)

v qr = Rr iqr + (ω − ωr)(Llr idr + Lm (ids + i dr)) + pλqr (12)

v dr = Rr idr − (ω − ωr)(Llr iqr + Lm (iqs + iqr)) + pλdr (13)

where Rr is rotor resistance, Rs is stator resistance, Lls is stator leakage inductance, L'lr is rotor leakage inductance, Lm is mutual inductance between stator and rotor winding, ω is the synchronous speed, ωr is the electrical speed of motor, and p denotes the time derivative. Also, here vqr = vdr = 0, since rotor bars are short-circuited.

The expression for the electromagnetic torque Tem is given by
Tem = 3/2 P/2 Lm [iqs i`dr − ids i`qr] (14)

Where, P is the number of poles.

The mechanical equation governing the OEWIM-pump drive is expressed as follows:

Tem = J dωrmech/dt + Bω2rmech + TL (15)

where J is motor inertia (kg-m2), B is centrifugal load torque coefficient, TL is load torque (N •m), and ωrmech is instantaneous angular velocity of motor shaft (rad/s).

III. OPERATION AND ANALYSIS OF THE PROPOSED SYSTEM:

The proposed dual inverter is operated by using the de-coupled PWM strategy. It incorporates simple V/f control for the efficient operation of system below the rated speed. The proposed PWM strategy requires the information of magnitude and angle of the reference voltage vector. The magnitude is calculated and controlled by the MPPT algorithm and the angle "α" is the function of time and fundamental frequency of reference

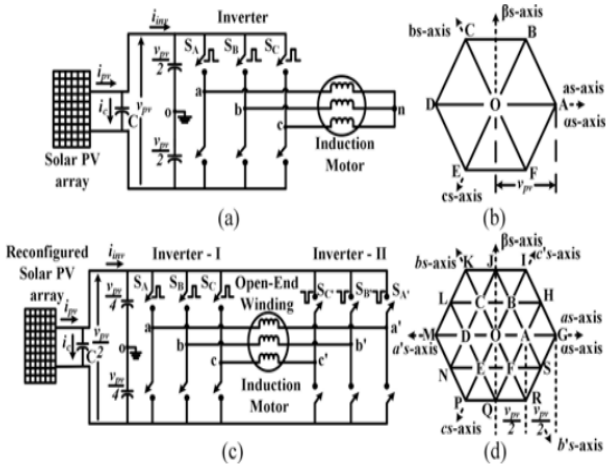

ISSN No: 2348-4845
International Journal & Magazine of Engineering, Technology, Management and Research
A Peer Reviewed Open Access International Journal

Fig. 4. Demonstration and comparison of dc-bus voltage requirement for Hbridge and dual-inverter systems. (a) Schematic circuit diagram of the two-level H-bridge inverter with input dc voltage (PV voltage) of "Vpv ." (b) Space vector locations of voltage vector obtained from two-level inverter. (c) Schematic circuit diagram of dual-inverter-fed OEWIM drive with input dc voltage (PV voltage) of "Vpv /2." (d) Space vector locations of voltage vector obtained from three-level dual-inverter scheme.

modulating waveform. The reference voltage vector |vsr|α is further divided into two decoupled components |vsr|/2 α and |vsr|/2 (180 + α). The decoupled components are then given as the reference vector for Inverters I and II, respectively, as shown in Fig. 2, for generation of required output voltage. Thus, using decoupled PWM configuration has the benefit of double output voltage.

A. Low Input DC-Bus Voltage Requirement of Dual Inverter for OEWIM-Pump Drive

To analytically verify the low input dc-bus voltage requirement, a comparison between two-level and dual-inverter-fed OEWIM is done. Both the inverters are compared for generating the same output voltage vector with different values of input PV source voltage. The low input voltage requirement of dual inverter for an OEWIM drive is demonstrated in Fig. 4. Let the PV source voltage required to generate the rated instantaneous IM phase voltage van is Vpv as shown in Fig. 4(a). From Fig. 4(a) and (b), the inverter output voltage, van , vbn , and vcn can be obtained using the inverter pole voltage, vao , vbo , and vco ; and switching functions SA , SB , and SC as follows:

$$Van = vao - vno = (2/3\ SA - 1/3\ (SB + SC)\ Vpv/2 \quad (16)$$

where vno is common-mode voltage given by

$$vno = 1/3\ (vao + vbo + vco) = 1/3\ (SA + SB + SC)\ Vpv/2 \quad (17)$$

Thus, the space vector location of reference voltage vector −→OA [see Fig. 4(b)] can be generated by the switching functions SA = 1, SB = −1, and SC = −1. Substituting these values into (17) will result in the phase voltage, van as 2Vpv /3. Now, consider the three-phase, three-level dual inverter connected to an OEWIM as shown in Fig. 4(c). Let the input PV source voltage is Vpv /2, which is half of the voltage taken for two-level H-bridge inverter.

Now, the dual inverter output phase voltage −−→OG [see Fig. 4(d)] is given as

$$Vaa` = vao - vao` - voo` \quad (18)$$

where voo is the common mode voltage [see Fig. 4(c)] which is given by

$$voo` = 1/3\ Vpv/4\ [(SA - SA`) + (SB - SB`) + (SC - SC`)]. \quad (19)$$

Therefore, vaa` is given by

$$Vaa` = [2/3\ (SA - SA`) - 1/3\ [(SB - SB`) + (SC - SC`)]]\ Vpv/4 . \quad (20)$$

So, to generate voltage vector −−→OG [see Fig. 4(d)], the switching functions required are SA = 1, SB = −1, and SC = −1; SA `= −1, SB` = 1, and SC` = 1. Substituting these values in (20), results in the phase voltage of magnitude 2Vpv /3 corresponding to phase aa'. Hence, to generate the phase voltage of 2Vpv /3, the PV source voltage required in case of two-level inverter is Vpv and in case of dual inverter connected to OEWIM is Vpv /2. However, the DSAZE PWM technique [22] needs excess 15% of dc-link voltage to generate the rated motor phase voltage.

IV. SIMULATION RESULTS:

Simulation is performed using MATLAB/SIMULINK software. Simulink liabrary files include inbuilt models of many electrical and electronics components and devices such as diodes, MOSFETS, capacitors, inductors, motors, power supplies and so on. The circuit components are connected as per design without error, parameters of all components are configured as per requirement and simulation is performed.

ISSN No: 2348-4845
International Journal & Magazine of Engineering, Technology, Management and Research
A Peer Reviewed Open Access International Journal

SIMULATION CIRCUIT:

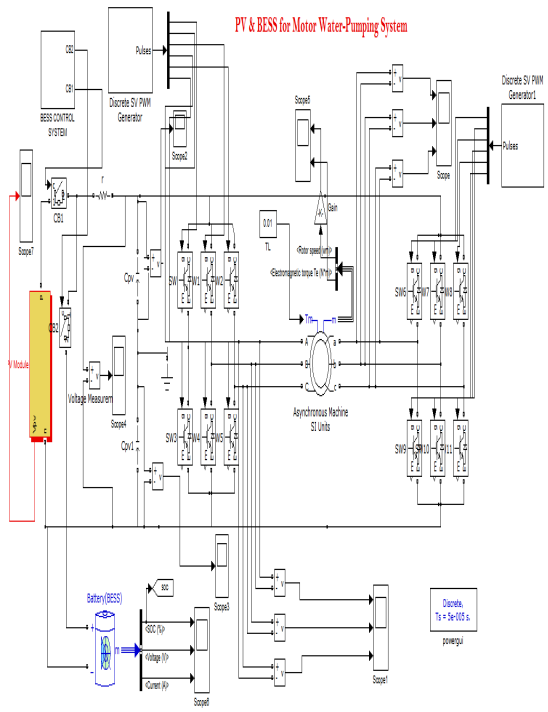

a)PV input

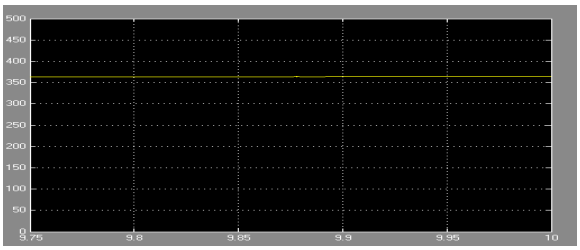

b)V C1

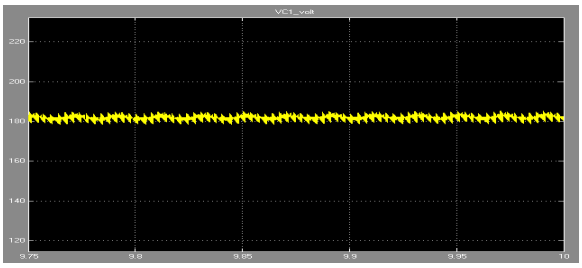

c)V C2

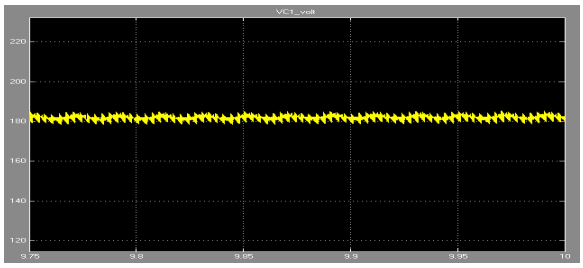

d)Inverter output

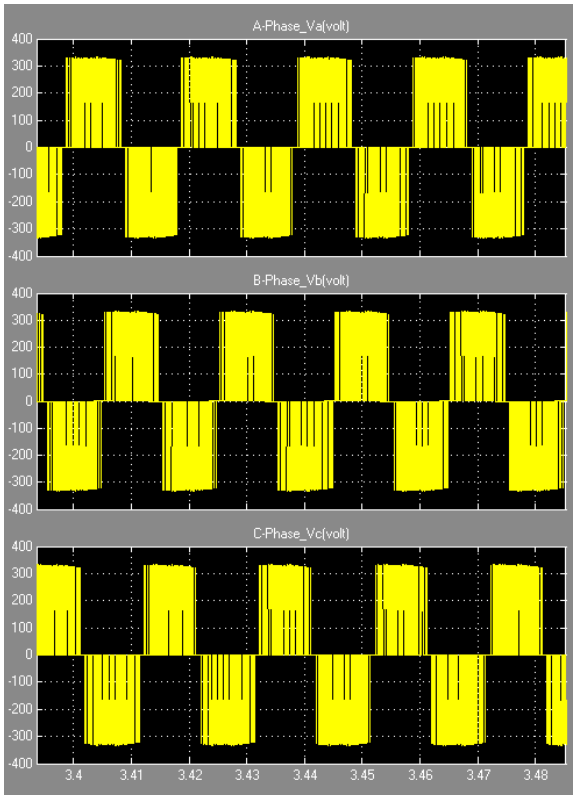

e)Speed & Torque

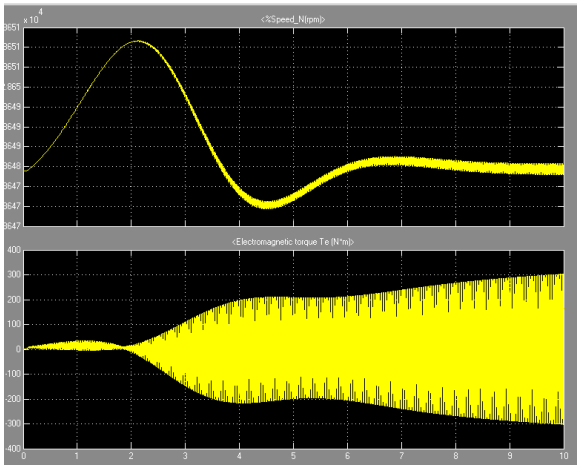

V. CONCLUSION:

This paper presents a solution for a photo-voltaic (PV) and battery energy storage- fed water-pump drive, which utilizes an open-end winding induction machine (OEWIM). The double inverter-bolstered OEWIM drive accomplishes the usefulness of a three-level inverter and obliges low esteem dc-transport voltage. This proposed inverter is simulated in MATLAB/SIMULINK software.

ISSN No: 2348-4845
International Journal & Magazine of Engineering, Technology, Management and Research
A Peer Reviewed Open Access International Journal

REFERENCES:

[1] D. Maheswaran, K. K. Jembu Kailas, V. Rangaraj, and W. Adithya Kumar, "Energy efficiency in electrical systems," in Proc. IEEE Int. Conf. Power Elect. Drives Energy Syst., Dec. 2012, pp. 1–6.

[2] Y. Yao, P. Bustamante, and R. S. Ramshaw, "Improvement of induction motor drive systems supplied by photovoltaic arrays with frequency control," IEEE Trans. Energy Convers., vol. 9, no. 2, pp. 256–262, Jun. 1994.

[3] J. V. Mapurunga Caracas, G. de Carvalho Farias, L. F. Moreira Teixeira, and L. A. de Souza Ribeiro, "Implementation of a high-efficiency, highlifetime and low-cost converter for an autonomous photovoltaic water pumping system," IEEE Trans. Ind. Appl., vol. 50, no. 1, pp. 631–641, Jan./Feb. 2014.

[4] J. Appelbaum, "Starting and steady-state characteristics of dc-motors powered by solar cell generators," IEEE Trans. Energy Convers., vol. EC-1, no. 1, pp. 17–25, Mar. 1986.

[5] S. M. Alghuwainem, "Steady-state performance of DC motors supplied from photovoltaic generators with step-up converter," IEEE Trans. Energy Convers., vol. 7, no. 2, pp. 267–272, Jun. 1992.

[6] S. R. Bhat, A. Pittet, and B. S. Sonde, "Performance optimization of induction motor-pump system using photovoltaic energy source," IEEE Trans. Ind. Appl., vol. IA-23, no. 6, pp. 995–1000, Nov./Dec. 1987.

[7] M. A. Vitorino and M. B. de Rossiter Correa, "An effective induction ˆ motor control for photovoltaic pumping," IEEE Trans. Ind. Electron., vol. 58, no. 4, pp. 1162–1170, Apr. 2011.

[8] S. Jain and V. Agarwal, "A single-stage grid-connected inverter topology for solar PV systems with maximum power point tracking," IEEE Trans. Power Electron., vol. 22, no. 5, pp. 1928–1940, Sep. 2007.

[9] L. H. S. C. Barreto, P. Peixoto Prac, D. S. Oliveira Jr., and R. N. A. L. Silva, "High-voltage gain boost converter based on three-state commutation cell for battery charging using PV panels in a single conversion stage," IEEE Trans. Power Electron., vol. 29, no. 1, pp. 150–158, Jan. 2014.

[10] M. A. Herran, J. R. Fischer, S. A. Gonz ´ alez, M. G. Judewicz, and D. ´ O. Carrica, "Adaptive dead-time compensation for grid-connected PWM inverters of single-stage PV systems," IEEE Trans. Power Electron., vol. 28, no. 6, pp. 2816–2825, Jun. 2013.

[11] B. N. Alajmi, K. H. Ahmed, G. P. Adam, and B. W. Williams "Singlephase single-stage transformer less grid-connected PV system," IEEE Trans. Power Electron., vol. 28, no. 6, pp. 2664–2676, Jun. 2013.

[12] Y. Zhou and W. Huang, "Single-stage boost inverter with coupled inductor," IEEE Trans. Power Electron., vol. 27, no. 4, pp. 1885–1893, Apr. 2012.

[13] S. Danyali, S. H. Hosseini, and G. B. Gharehpetian "New extendable single-stage multi-input dc-dc/ac boost converter," IEEE Trans. Power Electron., vol. 29, no. 2, pp. 775–788, Feb. 2014.

[14] . Sachin Jain, Athiesh Kumar Thopukara, Ramsha Karampuri, and V. T. Somasekhar, Member, IEEE. IEEE TRANSACTIONS ON POWER ELECTRONICS, VOL. 30, NO. 9, SEPTEMBER 2015